World Academy of Science, Engineering and Technology
International Journal of Materials and Metallurgical Engineering
Vol:6, No:5, 2012

Dye-Sensitized Solar Cell by Plasma Spray

*C.C. Chen, C.C. Wei, S.H. Chen, S.J. Hsieh, W.G. Diau

***Abstract*—**This paper aims to scale up Dye-sensitized Solar Cell (DSSC) production using a commonly available industrial material – stainless steel - and industrial plasma equipment. A working DSSC electrode formed by (1) coating titania nanotube (TiO_2 NT) film on 304 stainless steel substrate using a plasma spray technique; then, (2) filling the nano-pores of the TiO_2 NT film using a TiF_4 sol-gel method. A DSSC device consists of an anode absorbed photosensitive dye (N3), a transparent conductive cathode with platinum (Pt) nano-catalytic particles adhered to its surface, and an electrolytic solution sealed between the anode and the transparent conductive cathode. The photo-current conversion efficiency of the DSSC sample was tested under an AM 1.5 Solar Simulator. The sample has a short current (Isc) of 0.83 mA cm^{-2}, open voltage (Voc) of 0.81V, filling factor (FF) of 0.52, and conversion efficiency (η) of 2.18% on a 0.16 cm^2 DSSC work-piece.

***Keywords*—**DSSC, Spray, stainless steel, TiO_2 NT, efficiency

I. Introduction

DUE to increasing energy demands and environmental concerns about global warming, scientists are constantly looking for renewable energy sources. Sunlight is an abundant and clean energy source. Technologies for efficiently converting solar energy to electricity have undergone rapid development over the past few years. Within the area of nanotechnology, fabrication of functional nano-scale structures and devices in a well-controlled way is a grand challenge. Due to the small size of nano-elements, a bottom-up self-assembly process may be a viable approach to overcoming this challenge. For many years, titanium anodization has been used to improve the surface properties of metal for preventing corrosion and reducing wear and dents. This technique is also useful for development of new products such as capacitors or templates [1,2,3,4]. Recently, titanium oxides have been used for applications such as converting solar energy, photocatalytic syntheses, photocatalytic degradation of organic pollutants, and the electrolytic production of chlorine [5,6,7].

C.C. Chen. Department of Energy Engineering, National United University, 2, Lienda, Miaoli 36003 Taiwan (phone: +886-37-382383; fax:+886-37-382-391; e-mail: chentexas@gmail.com).

C.C. Wei., Department of Applied Chemistry, National Chiao Tung University, No.1001, Ta Hsueh Rd., Hsinchu 30010, Taiwan (e-mail: hattori0504.pas97g@gmail.com).

S.H. Chen. Department of Energy Engineering, National United University, 2, Lienda, Miaoli 36003 Taiwan (phone: +886-37-382383; fax:+886-37-382-391; e-mail: brucechen.mse90g@gmail.com).

S.J. Hsieh, Department of Engineering Technology and Department of Mechanical Engineering, Texas A&M University, College Station, TX 77843-3367(e-mail: hsieh@entc.tamu.edu).

W.G. Diau. Department of Applied Chemistry, National Chiao Tung University, No.1001, Ta Hsueh Rd., Hsinchu 30010, Taiwan (e-mail: diaue@mail.nctu.edu.tw).

Dye-sensitized solar cells (DSSCs) have become more attractive and received more attention than traditional monocrystalline silicon wafers, due to their relatively low materials cost and simple manufacturing process. A DSSC consists of an anode, electrolytic solution, and a cathode. A semiconductor layer is formed on the surface of the anode and photosensitive dyes are absorbed within. Owing to these features (low material cost and simple fabrication process), DSSCs are promising devices for commercialization [8, 9, 10, 11, 12]. More importantly, the cells are flexible, transparent and coloring, and bio-degradable; therefore, the cells can be mass produced and rolled into a roll, which takes less space. These features make DSSCs a cheaper alternative than silicon solar cells [13].

Currently the design of the electron-collecting layer (anode) of a DSSC cell is made of TiO_2 nanoparticles (NPs), following Gratzel's earlier design [8, 9]. However, NPs often slow down the diffusion process - electron transport - resulting in a lower light-to-electricity conversion efficiency in a NP-DSSC. To improve charge-collection efficiency (that is, to speed up electron transport and to slow down charge recombination), TiO_2 nanotubes (NTs) are fabricated as a film consisting of oriented one-dimensional (1D) nanostructures. The one-dimensional channel for carrier transportation is expected to reduce the amount of recombination of electron-holes (e^-/h^+). Zhu [14] has suggested that recombination in the NT films is ten times slower than in the NP films.

For a DSSC, the device resistance increases as the barrier layer thickness increases during the anodization process [15]-[17]. Poor contact at the Ti-TiO_2 NT interface during bending before anneal or increasing titanium oxides at Ti-TiO_2 NT interface during annealing [18] will reduce the fill factor. In contrast to anodic aluminum oxide (AAO) membrane [19], the weaker adhesion of TiO_2 NT on Ti and lower tube-to-tube adhesion results in the separation from the weak adhesion regions; therefore, this property limits the DSSC applications.

Moreover, the DSSCs that have TiO_2 nanotubes grown on Ti-foil requires back-side illumination; therefore, the devices have less power conversion efficiency than the DSSCs that require front-side illumination because Pt coated onto a transparent conduction oxide (TCO) and iodine electrolyte absorb only about 30% of incidental light [14]. For improving DSSC conversion efficiency, free-standing TiO_2 NT film has a higher power conversion efficiency than TiO_2 NT film on Ti substrate. This is because the front-side is illuminable and there is no barrier layer between the NT membrane and Ti substrate. Mor [20] and Paulose [21] fabricated TiO_2 NT film on fluorine-doped tin oxide (FTO) glass using sputter and anodization processes. Also, Albu [22], Chen [23], and Park [24] have described a process by which nanotube array films can be transformed into free-standing membranes.

II. Experiment Procedure

The pre-treatment process for 304 stainless steel (S. S.) substrate includes milling, sandblasting, and ethanol cleaning. A sample of 10cm×10cm×1cm 304 stainless steel was first subjected to a milling process to finish the surface. The sample was then sandblasted with 10~15 μm Al_2O_3 particles at a free-stream velocity of 5~20 m/s to achieve a roughness factor of Ra>4.0. Afterwards, a layer of 100μm ~300μm thickness of Ti film was deposited onto the roughened 304 stainless steel using a thermo plasma spray with 20-53 μm size Ti particles. A sample of 2.5cm×2.5cm×1cm 304 S. S. with Ti film was used as the DSSC anode substrate. The substrate with Ti film was then treated with anodization process, $TiCl_4$ treatment, and heat treatment to form anatase TiO_2 NT film, which becomes the anode of the DSSC.

The formula to grow TiO_2 NT is to use electrolyte with pH value of 6.8 of 0.5 wt.% ammonium fluoride (NH_4F, 99.9%) in a 2 wt.% H_2O in ethylene glycol ($C_2H_4(OH)_2$) solvent, and apply 1 hr potentiostat (60V), and 1 h galvanostat anodization (4.44 mA . cm^{-2}) for several stages of anodization. The substrate removed from the TiO_2 NT film was treated with titanium tetrafluoride (TiF_4). After TiO_2 NT samples were formed by anodization and TF_4 treatment, the samples were then annealed in an air furnace at 450℃ for 1 h to form anatase phase TiO_2 NT film. The unwanted surface deposits on the TiO_2 NT film introduced during anodization were removed effectively simply by ultrasonic cleaning in deionized water containing a small proportion of Al_2O_3 sub micrometer particles. After ultrasonic cleaning, a detailed micro-structure of compact film with nano-porous structures mixed with nanotubes was revealed. The DSSC anode was thus formed.

Indium doped tin oxide (ITO) glass coated with platinum (Pt) particles through a sputtering process was used as a counter electrode. Electrolyte containing 0.5 M lithium iodide (LiI) and 0.05M iodine (I_2) in acetonitrile (CH_3CN, 99.9%) was introduced into the electrodes. A DSSC device was built by assembling the two electrodes into a sandwich cell and then sealing the cell with a hot-melt film (SX1170, Solaronix, thickness 25 μm). Afterwards, a thin layer of electrolyte was introduced into the space between the two electrodes, and the conducting wires were attached to the anode and cathode using silver paste.

The N3 dye absorbed by the TiO_2 NT was measured using UV-visible-NIR spectrophotometers at room temperature. The photocurrent was produced using an HP model 4140B measuring unit. The N3 dye absorbed on the ATO was also measured using UV-visible-NIR spectrophotometers (Jasco, V-570) at room temperature. The photo-current conversion efficiency was tested under an AM 1.5 (300 W, 91160-Oriel Solar Simulator, 100 mw cm^{-2}) on a 0.16 cm^2 sample area.

III. Results and Discussion

Figure 1 shows a schematic diagram of the structure of a DSSC. For the anode, most DSSCs utilize TiO_2 film as a semiconductor layer coated on a conducting glass, such as indium tin oxide (ITO) glass. Sensitized dyes, such as N3 dye, are then absorbed on the TiO_2 film. For the cathode, platinum particles are coated on the conducting glass to serve as a catalyst for the iodine ions. The iodine-containing electrolyte is between the anode and cathode. The most used TiO_2 films include TiO_2 NPs film and TiO_2 NT film. Compared to the electron transfer in the TiO_2 NPs, the electrons transfer faster in the TiO_2 nanotubes (NTs). After irradiation by incidental light, the electrons of the photosensitive dye are excited from the ground state to the excited state in three stages: **(i)** The electrons transfer from the excited state of the photosensitive dye molecules to a conductive band of the semiconductor layer. The electrolytic solution is simultaneously oxidized, and the photosensitive dye is reduced. This process corresponds to holes transferring from photosensitive dye molecules to an electrolytic solution. **(ii)** The electrons in the semiconductor layer then transfer from a conductive layer to an external circuit and do work on external loads. **(iii)** The electrons return to the electrolytic solution from the external circuit via the cathode and reduce the electrolytic solution.

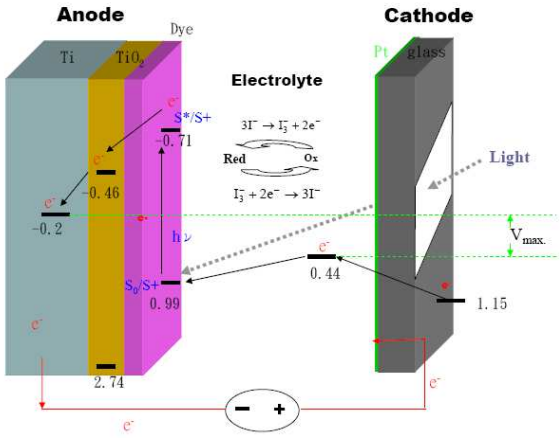

Fig. 1 Schematic diagram of DSSC energy levels when light irradiates the electrons transferring from dye → TiO_2 → Ti → external circuit and then via the cathode conductive layer back to the electrolyte

Figure 2 shows the fabrication procedure for TiO_2 NT on 304 Stainless Steel, starting with thermal spraying, TiF_4 treatment, and then anodization processes. The Ti film was first deposited onto the 304 Stainless Steel substrate using thermo-spraying; then the anodization process transforms partial Ti film to TiO_2 NT film. The large surface of thermo-spraying film plus the nano-structure of TiO_2 NT film offer a large surface area for hosting sensitized dye. The coated film always creates pore structures on the film. For example, Figure 3 shows how Ti film being deposited onto 304 S.S. substrate using the thermo-spray method. Titanium particles were melted using an arc gun and sprayed onto the 304 Stainless Steel substrate to form a layer of Ti film. A series of pores will be formed when Ti liquid drops are deposited and stacked on the substrate. The pores can create a short circuit between the cathode and anode substrate when electrolyte is between the layers. Therefore, these pores should be sealed, which can be achieved using TiF_4 sol-gel method. When TiF_4 solutions have a pH below 1.0 or a TiF_4 concentration below 0.03 M, neither precipitation nor film formation was observed. A large amount of precipitate was rapidly formed, and film was not deposited, on substrates above

pH 3.1. Therefore, the concentration of TiF_4 should be controlled above 0.03M, and the pH value should be controlled between 1 and 3 so that TiO_2 nanoparticles can be formed and be deposited on the substrate.

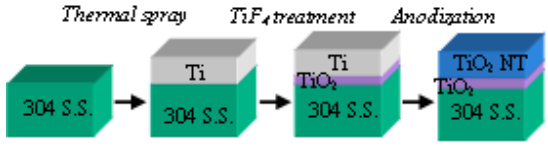

Fig. 2 Fabrication procedure for TiO_2 NT on 304 S.S. showing thermal spray, TiF_4 treatment, and anodization processes

Figure 4 uses optical images to show process of making DSSC anode. Figure 4(a) shows the effect of sandblasting to improve 304 S.S. substrate surface roughness so that the surface is clean and rough for Ti film adhesion. Figure 4(b) shows Ti film applied on 304 S.S. substrate by thermo-spraying. The film is continuous and dense to allow TiO_2 NT formation. Figure 4(c) shows TiO_2 NT formation by anodization; the film offers a large surface for sensitized dye absorption. Figure 4(d) shows anatase TiO_2 NT formation by annealing and the film which is suitable for electron transportation. Figure 5 shows optical images of Ti film fabricated using the thermo-spray process; 5(a) is a top view of the rough surface; 5(b) shows the laminar structure of Ti film with 200μm thickness on the 304 S.S. substrate. Figure 6 shows SEM images of Ti film fabricated using the thermo`-spray process; 6(a) shows several μm diameter size Ti drops on the Ti film, and 6(b) shows a zoomed-in view of the Ti drops. Both Ti drop and film can provide a surface for TiO_2 NT formation.

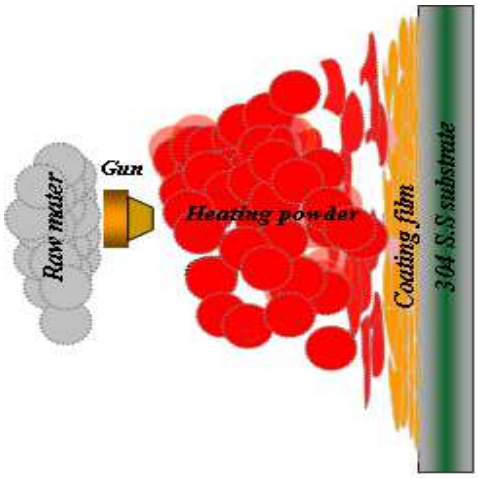

Fig. 3 Schematic diagram of Ti film on 304 S.S. substrate using thermo-spray method

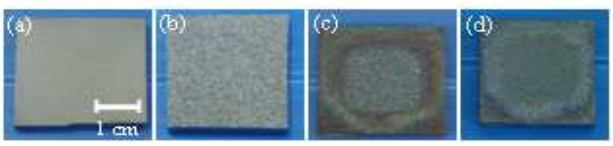

Fig. 4 Optical images of (a) sandblasting 304 S.S., (b) Ti film on 304 S.S. substrate by thermo-spray, (c) TiO_2 NT formation by anodization, (d) anatase TiO_2 NT formation by annealing

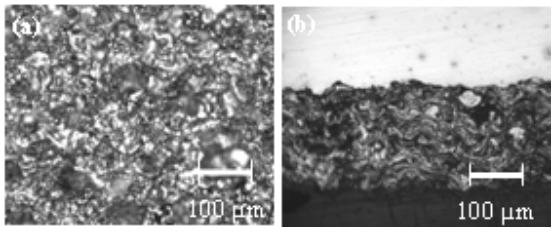

Fig. 5 Optical images of Ti film fabricated using thermo-spray process, (a) top view and (b) side view

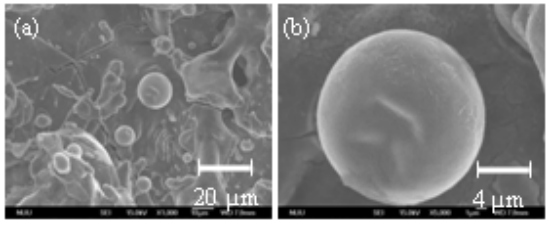

Fig. 6 SEM images of Ti film fabricated using thermo-spray process; (a) Ti drops and Ti film, and (b) zoomed-in view of Ti drops

Figure 7 shows SEM images of TiO_2 NT film fabricated by anodization on thermo-spray Ti film. In (a), the anodic titanium oxide structure is not just a nanotube, but a compact film on the surface. The unwanted surface deposits on the films introduced during anodization were removed effectively simply by ultrasonic cleaning in deionized water containing Al_2O_3 as sub-micrometer particles in a small proportion. (b) After ultrasonic cleaning, a clean TiO_2NT film was presented. Figure 8 shows SEM images of TiO_2 NT film fabricated by anodization on thermo-spray Ti film; (a) shows film, drop, and particle surface formations of TiO_2 NT, (b) zoomed in view of particle surface, (c) TiO_2 NT formation on Ti drop, (d) zoomed in view of drop surface, (e) TiO_2 NT formation on film, (f) zoomed in view of film surface. Based on these SEM images, the TiO_2 NT have ordered pores with 100 nm pore diameter, 140 nm pore distance and 20 nm pore wall thickness, and 5×10^9 pore cm^{-2}. Figure 9 shows the DSSC cell performance under simulated AM 1.5 light tests. (a) Absorption spectrum: the N3 dye absorbance ranges from 350 nm to 800 nm, and two absorbance peaks of 410 nm and 535 nm were present at the absorbance curve. (b) Current–voltage (J-V) curve of photocurrent efficiency: The DSSC device has a short current (Isc) of 0.83 mA cm^{-2}, open voltage (Voc) of 0.81V, fill factor (FF) of 0.52, and conversion efficiency (η) of 2.18% on a 0.16 cm^2 DSSC sample.

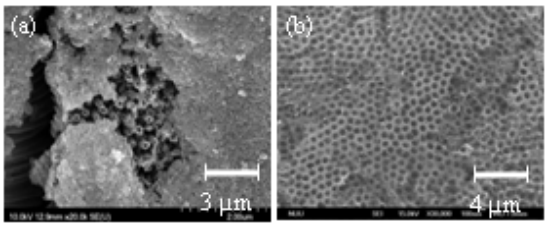

Fig. 7 SEM images of TiO_2 NT film fabricated by anodization on thermo-spray Ti film; (a) compact layer on the NT film before ultrasonic treatment, and (b) clean NT film after ultrasonic treatment

IV. Conclusion

Having a large surface area of nanoporous TiO_2 film enhances electrochemical reaction efficiency. A large area DSSC anode was made by thermo-spraying Ti on 304 S.S substrate and using anodization to form TiO_2 NT as an electron transport film, and the performance of the device was measured at 2.18% conversion efficiency. The process of using thermo-spraying and anodization to fabricate industry-scale oxide film production is novel. This work aims to transfer nanotechnology discoveries from the laboratory to industrial application and to scale up DSSC fabrication for high-rate production.

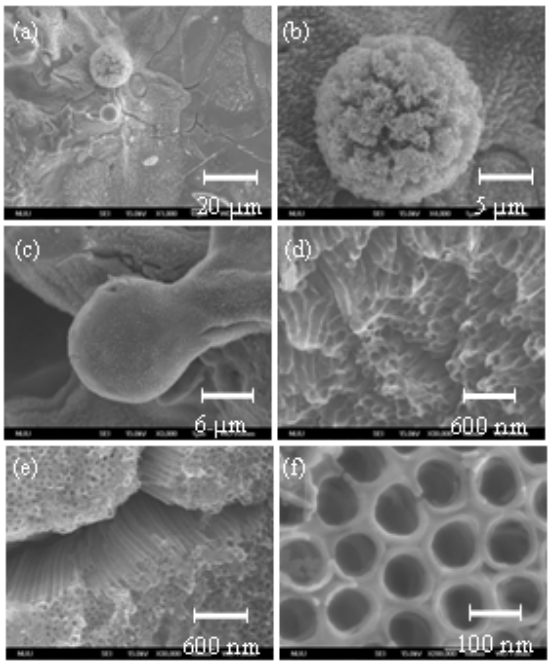

Fig. 8 SEM images of TiO_2 NT film fabricated by anodization on thermo-spray Ti film; (a) TiO_2 NT film, drop, and particle surface formations, (b) zoomed in view of particle surface, (c) TiO_2 NT formation on Ti drop, (d) zoomed in view of drop surface, (e) TiO_2 NT formation on the film, (f) zoomed in view of film surface

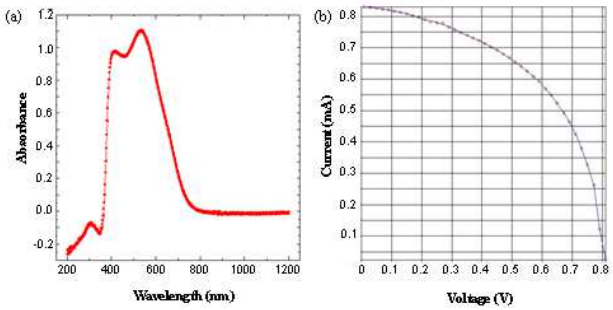

Fig. 9 DSSC cell performance: (a) absorption spectrum and (b) current–voltage (J-V) curve of photocurrent efficiency

Acknowledgment

This study was partially supported by a grant from the National Science Council, Taiwan (100-2918-I-239-001).

References

[1] Y.T. Sul, C.B. Johansson, Med. Eng. Phys. 23 (2001) 329.
[2] H. Habazaki, M. Uozumi, Electrochem. Acta 47 (2002) 3837.
[3] F. Schlotting, J. Schreckenbach, Appl. Surf. Sci. 90 (1995) 129.
[4] D. Gong, C.A. Grimes, O.K. Varghese, Z. Chen, W.C. Hu, E.C. Dickey, J. Mater. Res., 16 (2001) 3331.
[5] R. Wang, K. Hashimoto, Nature 388 (1997) 431.
[6] M. Gratzel, Nature 409 (2001) 575.
[7] T. Ohtsuka, T. Otsuki, J. Electroanal. Chem. 473 (1999) 272.
[8] O'Regan, B.; Grätzel, M. Nature 1991, 353, 737.
[9] Grätzel, M. Nature 2001, 414, 338.
[10] Nazeeruddin, M. K.; Angelis, F. D.; Fantacci, S.; Selloni, A.; Viscardi, G.; Liska, P.; Ito, S.; Takeru, B.; Grätzel, M. J. Am. Chem. Soc. 2005, 127, 16835.
[11] Wei, M.; Konishi, Y.; Zhou, H.; Yanagida, M.; Sugihara, H.; Arakawa, H. J. Mater. Chem. 2006, 16, 1287.
[12] Koide, N.; Islam, A.; Chiba, Y.; Han, L. J. Photochem. Photobio. A 2006, 182, 296.
[13] Kong, F. T.; Dai, S. Y.; Wang, K. J. Advances in Opto Electronics 2007, 1.
[14] Zhu, K.; Neale, N. R.; Miedaner, A.; Frank, A. J. Nano Lett. 2007, 7, 69.
[15] Gong, D.; Grimes, C. A.; Varghese, O. K.; Chen, Z.; Hu, W. C.; Dickey, E. C. J. Mater. Res. 2001, 16, 3331.
[16] Cai, Q.; Paulose, M.; Varghese, O. K.; Grimes, C. A. J. Mater. Res. 2005, 20, 230.
[17] Grimes, C. A. J. Mater. Chem. 2007, 17, 1451.
[18] Chen, C. C.; Diau, E. W. G.; Hsieh, S. J.; Say, W. C. Applied Physics A 2009, Accepted.
[19] Chen, C. C.; Chen, J. H.; Chao, C. G. Jpn. J. Appl. Phys. 2005, 44, 1529.
[20] Mor, G. K.; Shanka, K.; Paulose, M.; Varghese, O. K.; Grimes, C. A. Nano Lett. 2006, 6, 215.
[21] Paulose, M.; Prakasam, H. E.; Varghese, O. K.; Peng, L.; Popat, K. C.; Mor, G. K.; Desai, T. A.; Grimes, C. A. J. Phys. Chem. C 2007 111,14992.
[22] Albu, S.P.; Ghicov, A.; Macak, J. M.; Hahn, R.; Schmuki, P. Nano Lett. 2007, 7, 1286.
[23] Chen, Q.; Xu, D.; Wu, Z.; Liu, Z. Nanotechnology 2008, 193, 65708.
[24] Park, J. H.; Lee, T. W.; Kang, M. G. Chem. Comm. 2008, 2867.